THE JOURNAL OF PHYSICAL CHEMISTRY B

Article

pubs.acs.org/JPCB

Crucial Importance of Water Structure Modification on Trimethylamine *N*-Oxide Counteracting Effect at High Pressure

Rahul Sarma and Sandip Paul*

Department of Chemistry, Indian Institute of Technology, Guwahati Assam, India-781039

Supporting Information

ABSTRACT: Penetration of water molecules into the protein interior under high hydrostatic pressure conditions, leading to protein structural transition, is a well-known phenomenon. The counteracting effect of a naturally occurring osmolyte, trimethylamine *N*-oxide (TMAO), against pressure-induced protein denaturation is also well-established. But, what is largely unknown is the mechanism by which TMAO counteracts this protein denaturation. So to provide a molecular level understanding of how TMAO protects proteins at high pressure, we report here molecular dynamics (MD) computer simulation results for aqueous solutions of *N*-methylacetamide (NMA) with different TMAO concentrations over a wide range of pressures relevant to protein denaturation. Hydration behavior of NMA is analyzed at different conditions chosen. It is observed that hydrostatic pressure leads to a significant compression of hydration shell of nonpolar groups and increases hydration number. The compression is relatively insignificant in the vicinity of hydrogen bonding sites. TMAO can prevent pressure-induced enhanced hydration of NMA molecules. Interaction of TMAO with NMA and the structural and dynamical properties of water (site−site radial distribution function, coordination number, hydrogen-bond number, and lifetime) are also investigated to find the origin of the counteracting action of TMAO. Our results confirm that TMAO and pressure have counteracting effects on the water structural and dynamical properties, giving an explanation as to how TMAO counteracts pressure-conferred denaturation of proteins.

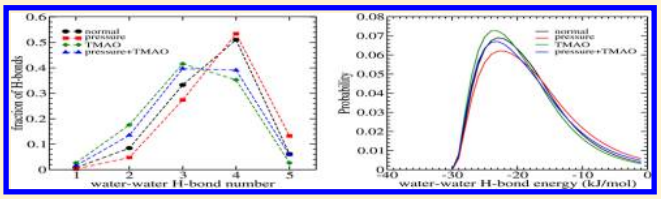

I. INTRODUCTION

The naturally occurring osmolyte, trimethylamine *N*-oxide (TMAO), is well-known for its ability to stabilize proteins[1,2] and nucleic acids,[3] correct medicinally significant issues such as prion aggregation[4] and cellular folding defects,[5] and protect proteins in perturbing conditions.[6−10] Protein response to high hydrostatic pressures in the presence of TMAO has received particular attention in recent years.[6,9,10] Yancey reported a linear increase of TMAO concentration with depth of the sea both among different species and within the same species.[6] The common osmolytes of shallow relatives, e.g., urea in skates, were replaced by high levels of TMAO and the typical 2:1 concentration ratio of urea to TMAO in shallow elasmobranchs was found to be altered by a 1:2 urea:TMAO ratio in a species from 3 km depth.[6] These findings led Yancey to suggest that TMAO might act as a pressure counteractant. Indeed, the counteracting effect of TMAO against high pressure has been extensively confirmed in a variety of protein systems. TMAO was observed to offset pressure-inhibition of stability of several lactate dehydrogenase homologous, polymerization of actin, enzyme−substrate binding for two enzymes and growth of living yeast cells.[6] Recent small-angle X-ray scattering (SAXS) studies also provided evidence for the counteracting effect of TMAO against pressure.[9,10]

The molecular level picture by which TMAO offset pressure-induced protein denaturation is not clear yet. A large number of studies have been devoted to understand the mechanism of protein stabilization at ambient pressure conditions and there are several excellent experimental and theoretical articles published in this area. TMAO interaction with the peptide backbone through its hydrated form has been reported in the literature[11−13] and there is general agreement on preferential exclusion of this osmolyte from the protein surface.[1,14−19] TMAO was also shown to have negligible effect on hydrophobic interaction of small molecule.[20,21] What is more, TMAO can interact strongly with water to form di- and/or trihydrated TMAO complexes in solution.[22−25] So a physical model for TMAO-induced protein stabilization and counteraction can be posited in which direct TMAO−water interaction reduces availability of water to solvate protein residues. TMAO effect on protein hydration through its indirect effect on water structure has also been proposed.[22,23,25−31] However, the usefulness of the water structure perturbation ideas in predicting the protein stability is a controversial issue. In their simulation study, Zou et al. observed enhancement of water structure by TMAO in the form of a slight increase in the number of hydrogen bonds per water molecule, stronger water hydrogen bonds, and long-range spatial ordering of the solvent, suggesting protein stabilization by enhancement of water structure.[22] On the other hand, the simulation study by Athawale et al. indicated that different measures of "water structure" can display opposite trends in the presence of

Received: November 9, 2012
Revised: December 25, 2012
Published: December 27, 2012

TMAO.[20] Similarly, computations of hydrogen bond number provided no evidence for an increase in the water structure in binary aqueous TMAO solution or in a mixture of urea/TMAO solution.[32] Thus, there are clear discrepancies in simulation studies that investigate indirect effect of TMAO on the solvent and hence further investigation is needed. Moreover, rather than extrapolating the results from ambient pressure conditions to high pressure conditions, it is expedient to focus on TMAO systems under high pressure conditions for a better interpretation of the counteracting mechanism.

Again, water has long been known to play a key role in governing the structures, stability, dynamics, and functionality of proteins[33−35] and, in fact, penetration of water molecules into the protein interior at high pressure was suggested to be a primary driving force for pressure-induced protein structural transition.[36−46] In a series of studies by Kinoshita and his co-workers, it was argued that water molecules in the bulk are extremely crowded at high pressure and penetration into the protein interior increases their total entropy in the system, favoring the pressure-denatured structure.[47−49] Significant collapse of water second shell was seen in some recent studies.[50,51] Using SAXS in combination with a liquid state theoretical approach, Schroer et al. studied the influence of pressure on the structure and protein−protein interaction potential of dense protein solutions.[52] They reported that the structural change of water at high pressure lead to a modification of the structure and intermolecular interaction potential of the protein lysozyme. On these grounds, it is reasonable to assume that water penetration is associated with structural change of water caused by high hydrostatic pressures. Then, the question that arises naturally is, can TMAO prevent the pressure-induced modification of water structure? In shedding light on the counteracting action of TMAO, this is not a trivial question at all and this is the primary concern in the present study.

In a recent article, we discussed the effects of pressure on the solution structure and hydrogen bond properties of *N*-methylacetamide (NMA), the smallest amide that represents both hydrophobic and hydrogen bonding sites in proteins, in pure water.[53] Herein, we present molecular dynamics (MD) simulation results of NMA in aqueous solutions containing different TMAO contents as well as in pure water over a wide range of pressures. The goal is to understand the mechanism by which TMAO counteracts pressure-induced protein denaturation. To provide a sufficient number of NMA solvation sites for water and TMAO molecules avoiding NMA−NMA hydrogen bonds as much as possible, dilute NMA solutions are used in this study. The systems considered here, therefore, have negligible number of NMA−NMA hydrogen bonds (Figure 1 in Supporting Information) and represent typical solvent-exposed states of proteins where protein backbone can form hydrogen bonds easily with solution species. First of all, we examine the hydration behavior of NMA in pure water system at 1 atm and then extend it to systems with high pressure and high TMAO concentration to see how hydration of NMA sites is affected by pressure and what is the role of TMAO on this pressure-induced modification of NMA hydration. Solvation of NMA by TMAO is then examined. This is followed by investigation of water structure in these different solution conditions. The familiar water oxygen−oxygen radial distribution function is used to describe water structuring. The hydrogen bond properties and dynamics of water molecules are also studied and the influence of increasing TMAO concentration on water structural and dynamical properties with increasing pressure is discussed.

The remainder of this article is organized into three parts. The models and simulation details are briefly described in section II, the results are discussed in section III, and our conclusions are summarized in section IV.

II. MODELS AND SIMULATION METHOD

To understand the mechanism of protein protection by the osmolyte TMAO against pressure denaturation, we carried out classical MD simulations of NMA in pure water as well as in binary TMAO solutions of increasing concentrations at five different hydrostatic pressures ranging from 1 to 8000 atm. Twenty NMA molecules (mole fraction of 0.04) were used in each simulated system and the concentration of TMAO in these systems varied from 0 to 4 M. An overview of simulations is presented in Table 1. Note that the total number of molecules was fixed at 500 in all cases and, though the central simulation cell for the NMA−water system contained 20 NMA molecules immersed in 480 water molecules, TMAO solutions were constructed by replacing water molecules with TMAO. We used the popular extended simple point-charge (SPC/E) model[54] for water and described TMAO and NMA with rigid version of models proposed by Kast et al.[55] and Jorgensen and Swenson,[56] respectively. The interaction between atomic sites of two different molecules was expressed as

$$u_{\alpha\beta}(r_{\alpha\beta}) = 4\varepsilon_{\alpha\beta}\left[\left(\frac{\sigma_{\alpha\beta}}{r_{\alpha\beta}}\right)^{12} - \left(\frac{\sigma_{\alpha\beta}}{r_{\alpha\beta}}\right)^{6}\right] + \frac{q_\alpha q_\beta}{r_{\alpha\beta}} \quad (1)$$

where $r_{\alpha\beta}$ is the distance between atomic sites α and β, and q_α is the charge of the site α. The Lennard-Jones (LJ) parameters $\sigma_{\alpha\beta}$ and $\varepsilon_{\alpha\beta}$ were obtained by using the combining rules $\sigma_{\alpha\beta} = (\sigma_\alpha + \sigma_\beta)/2$ and $\varepsilon_{\alpha\beta} = (\varepsilon_\alpha\varepsilon_\beta)^{1/2}$. The values of the LJ parameters and

Table 1. Overview of Simulations[a]

system	P (MPa)	V (nm^3)	N_s	N_t	N_w	x_t
S1	0.1	16.77	20	0	480	0
S1	200	15.57	20	0	480	0
S1	400	14.95	20	0	480	0
S1	600	14.36	20	0	480	0
S1	800	13.91	20	0	480	0
S2	0.1	18.10	20	20	460	0.04
S2	200	16.95	20	20	460	0.04
S2	400	16.20	20	20	460	0.04
S2	600	15.67	20	20	460	0.04
S2	800	15.23	20	20	460	0.04
S3	0.1	18.78	20	30	450	0.06
S3	200	17.65	20	30	450	0.06
S3	400	16.90	20	30	450	0.06
S3	600	16.31	20	30	450	0.06
S3	800	15.86	20	30	450	0.06
S4	0.1	19.65	20	40	440	0.08
S4	200	18.33	20	40	440	0.08
S4	400	17.56	20	40	440	0.08
S4	600	16.94	20	40	440	0.08
S4	800	16.52	20	40	440	0.08

[a] V, N, and x represent box volume, number of molecules and mole fraction, respectively. Subscripts s, w, and t refer to solute (NMA), water, and TMAO.

dx.doi.org/10.1021/jp311102v | J. Phys. Chem. B 2013, 117, 677−689

the partial charges for NMA, TMAO, and water are summarized in Table 2.

Table 2. Lennard-Jones Parameters and Charges for the Models Considered[a]

	atom type	σ (Å)	ε (kJ/mol)	charge (e)
water	O_w	3.166	0.646	−0.8476
	H_w			+0.4238
NMA	C	3.75	0.439	+0.50
	O	2.96	0.878	−0.50
	N	3.25	0.711	−0.57
	H	0.0	0.0	+0.37
	$Me_1(CH_3-C)$	3.91	0.669	0.0
	$Me_2(CH_3-N)$	3.80	0.711	+0.20
TMAO	C_t	3.041	0.281	−0.26
	N_t	2.926	0.8314	+0.44
	O_t	3.266	0.6344	−0.65
	H_t	1.775	0.0769	+0.11

[a] e is the elementary charge.

All MD simulations were performed at 298 K in a cubic box of length L. The LJ interactions were spherically truncated at a radius of $L/2$ and the Ewald method[57] was used to treat the long-range electrostatic interactions. The quaternion formulation of the equations of rotational motion was employed and for time integration, we used leapfrog algorithm with a time step of 10^{-15} s. Periodic boundary condition and minimum image convention were used. Initially, the average volume of the simulation box corresponding to the desired pressure was determined by performing simulation in isothermal−isobaric ensemble (NPT). The weak coupling scheme proposed by Berendsen et al.[58] was used to maintain the physical pressure. During this period, the box volume was allowed to fluctuate. The so obtained box volume was used in subsequent canonical ensemble (NVT) simulation runs. Each system was equilibrated with velocity rescaling to fix the temperature. Finally, production runs were carried out for 10 ns and these are the results reported.

III. RESULTS AND DISCUSSION

A. Hydration of NMA. To obtain molecular details of NMA hydration at different pressures and TMAO concentrations, site−site radial distribution functions (rdfs) ($g_{\alpha\beta}$) among different atomic sites of NMA and water were computed. For a further analysis, we also calculated the average number of water molecules around these atomic sites using the relation

$$n_{\alpha\beta} = 4\pi\rho_\beta \int_0^{r_c} r^2 g_{\alpha\beta}(r)\, dr \qquad (2)$$

where $n_{\alpha\beta}$ represents the number of atoms of type β surrounding atom α in a shell extending from 0 to r_c and ρ_β is the number density of β in the system.

The hydration pattern of the carbonyl methyl group (Me_1) in pure water at 1 atm exhibits surface parallel orientation of water molecules around this hydrophobic group. It is adequately described by the site−site Me_1-O_w and Me_1-H_w rdf profiles with first peaks at similar positions (Figure 1). There is also a tail of hydrogen density at shorter separation, which reflects a slight preference of water hydrogens to come closer to the nonpolar surface. This behavior of water molecule is typical of hydrophobic hydration.[20,21] As depicted in Figure 1, the water

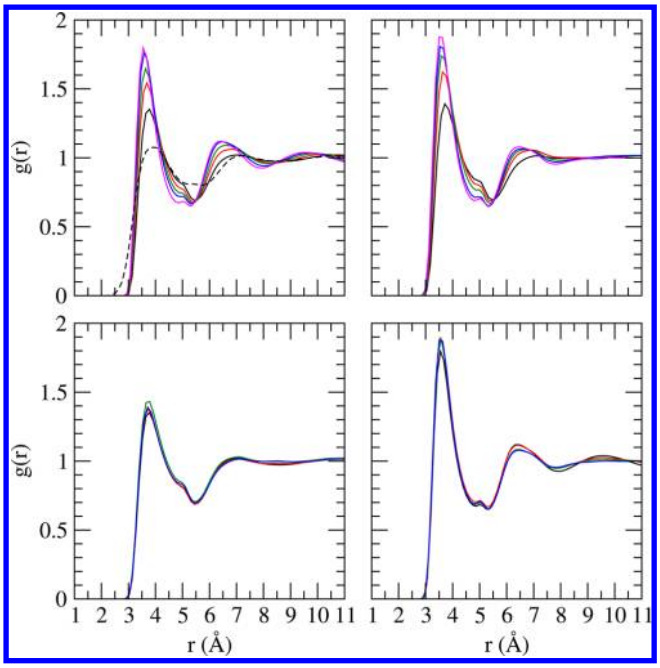

Figure 1. Site−site distribution functions involving NMA methyl group (Me_1) and water oxygen (O_w) as a function of pressure (top panel) for systems S1 (left) and S4 (right) and also as a function of TMAO concentration (bottom panel) for 1 (left) and 8000 (right) atm pressures. For top panel, black, red, green, blue, and magenta lines are for 1, 2000, 4000, 6000, and 8000 atm, respectively, whereas black, red, green, and blue lines in bottom panel represent systems S1, S2, S3, and S4, respectively. The dashed line is for water hydrogen (H_w).

distribution around Me_1 group is not as defined as that around a methane molecule.[21] This perturbation of water structure around NMA hydrophobic surface is supported by the findings that the solvent density around a methyl group in ethane is somewhat less layered than the solvent density around a methane molecule and also that water peaks are narrower and sharper for spherical molecules (methane, isobutane, neopentane) than those for nonspherical molecules (ethane, propane, n-butane).[59,60] For the pure buffer, integration of the rdf to 4.0 Å yields 4.9 water molecules around Me_1 group.

The second methyl group in NMA (Me_2) exhibits similar hydration characteristics (Figure 2). However, the water distribution is slightly better defined in the vicinity of this group as revealed by an increase in first peak height and an inward movement of the first minimum in Me_2-O_w rdf. The hydration number for this methyl group, obtained by integrating the rdf to 4.0 Å, is found to be 5.4, which is slightly higher than that for Me_1 group.

Increasing the pressure from 1 to 8000 atm leads to a significant modification of water distribution in the vicinity of NMA methyl groups. The water exclusion radius (the smallest distance at which $g(r) = 1$) decreases under pressure. This decrease, although it can be seen also at 2000 atm, is easily visible at 8000 atm. At the same time, the first maximum and minimum shift to shorter distances, indicating inward movement of first hydration shell. For the amide methyl group, which has a relatively well-defined first hydration shell at 1 atm, the positions of the first peak and minimum at 8000 atm are ≈0.2 and ≈0.3 Å inward than those at 1 atm. Inward movements are observed also for successive hydration layers. These observations are clear indicators of highly compressed water shell in the vicinity of nonpolar groups. What seems to be

dx.doi.org/10.1021/jp311102v | J. Phys. Chem. B 2013, 117, 677−689

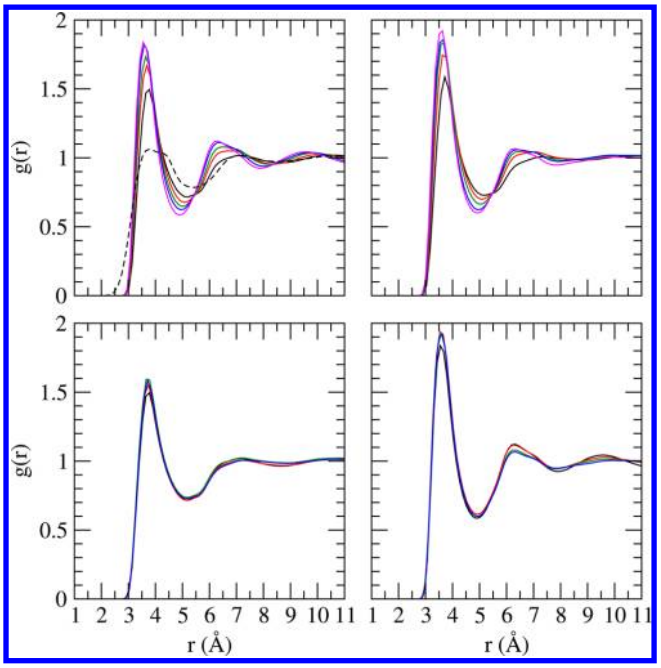

Figure 2. As in Figure 1 except for the Me_2 group of NMA.

more interesting is the monotonic increase in water density at the center of each hydration shell (the peak) and its decrease at the position which separates two hydration layers. These results imply a movement of water molecules from the large-*r* side in a particular shell toward its short-*r* side. The water movement under pressure thus leads to a reduction in empty spaces in the vicinity of hydrophobic group with higher water density in this region and also makes the hydration shell more structured. Because existence of well-defined hydration layer surrounding a solute is directly related to its dissolution, solvent separation of hydrophobic contacts at high pressure becomes clear from these results. Note that more efficient packing of water molecules around hydrophobic solute at high pressures and consequent pressure-induced relative stabilization of the water-separated configuration of nonpolar solute as compared to its associated state have been reported in the literature.[37,61−63]

The average numbers of water molecules around selected atomic sites in NMA at different perturbing conditions chosen are assembled in Table 3. As expected from the behavior of methyl−water rdf, which shows a monotonic increase in the height of the first peak with pressure with significantly compressed water shell, the average number of water molecules in the close proximity of methyl group increases as the pressure is increased. It can be seen that, in the absence of TMAO, as pressure increases from 1 atm through 4000 to 8000 atm, the hydration number for Me_1 increases from 4.9 through 6.5 to 7.7. So, at 8000 atm, there is about 57% increase in hydration number. Similarly, for Me_2 group, high hydrostatic pressure (8000 atm) leads to about a 52% increase (from 5.4 to 8.2) of the hydration number. These observations are in good agreement with general findings that high pressure structures of proteins have more water molecules in its interior than the low pressure structures.[44]

TMAO affects water distribution near NMA methyl group only slightly (Figures 1 and 2). The only notable feature about TMAO effect is the prevention of a more structured second hydration shell of methyl groups at high pressure. Although the water density in the vicinity of a methyl group is not affected by

Table 3. Hydration Characteristics of Selected Atomic Sites in NMA[a]

system	*P* (MPa)	Me_1	Me_2	O	H
S1	0.1	4.9	5.4	3.8	4.2
S1	200	6.3	6.8	4.7	5.0
S1	400	6.5	7.0	4.8	5.0
S1	600	6.8	7.2	5.1	5.1
S1	800	7.7	8.2	5.6	5.7
S2	0.1	4.3	4.8	3.2	3.8
S2	200	5.6	6.1	4.0	4.5
S2	400	5.9	6.3	4.2	4.6
S2	600	6.8	7.2	4.7	5.1
S2	800	7.1	7.6	5.0	5.3
S3	0.1	3.7	4.2	2.8	3.4
S3	200	4.8	5.2	3.4	3.9
S3	400	5.1	5.5	3.6	4.1
S3	600	6.1	6.5	4.2	4.7
S3	800	7.0	7.4	4.7	5.2
S4	0.1	3.7	4.2	2.7	3.4
S4	200	4.1	4.5	2.9	3.5
S4	400	5.1	5.6	3.5	4.1
S4	600	6.1	6.4	4.0	4.6
S4	800	6.2	6.5	4.1	4.6

[a]The hydration numbers are obtained by integrating the rdf to 4.0 Å.

TMAO, it indeed reduces the average hydration number of the hydrophobic moiety (Table 3). For the highest TMAO concentration considered (system S4), a 24% decrease of the average hydration number of the carbonyl methyl group (from 4.9 for S1 to 3.7 for S4) at 1 atm is observed in this study. The hydration number of methyl group is largely dependent on TMAO concentration at a particular pressure.

Figures 3 and 4 exhibit hydration characteristics of the two possible hydrogen bonding sites in NMA. We can expect the amide nitrogen of NMA to donate its hydrogen to water oxygen ($NH\cdots O_wH_w$) and the carbonyl oxygen to act as proton acceptor from the water oxygen ($CO\cdots H_wO_w$). This hydrogen bonding interaction, which should lead to different orientational behavior of water molecules near the carbonyl oxygen and amide hydrogen, is demonstrated in rdf profiles of NMA oxygen and hydrogen atoms. In particular, for pure water at 1 atm, the contact peaks in $O-H_w$ and $O-O_w$ rdf profiles, which characterize the first neighbor, appear at about 1.8 and 2.8 Å, respectively, reflecting formation of hydrogen bond between carbonyl oxygen and water. On the contrary, as reflected in the peak positions (O_w followed by H_w), water oxygen is preferred near the amide hydrogen and water oxygen accept this amide hydrogen in NMA−water hydrogen bonding interaction (the first peak appears at the characteristic location of hydrogen bond formation). Considering the effect of pressure alone, i.e., in the absence of TMAO, we find that the first peak in $O-H_w$ and $H-O_w$ rdf profiles does not change its location on application of pressure and the peak height reduces slightly. Also, the first minimum shows an upward movement. The $O-O_w$ rdf follows similar trends with a much more pronounced upward movement at high pressure. These findings reveal a tendency of part of the hydration water to move toward large-*r* side of the first shell at high pressure. This behavior is quite different from that in the vicinity of nonpolar surfaces where water molecules move from large-*r* side of the first shell toward its short-*r* side. Hence, the water shell is much more compressed in the vicinity of nonpolar groups relative to the

dx.doi.org/10.1021/jp311102v | J. Phys. Chem. B 2013, 117, 677−689

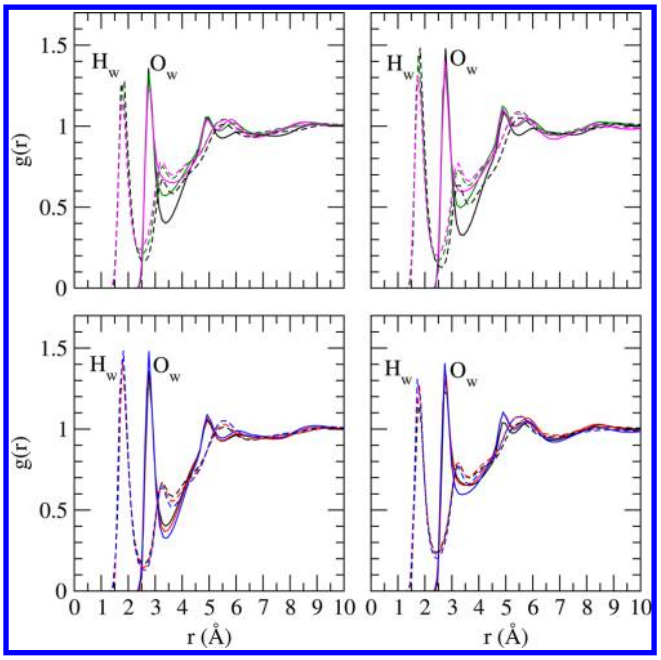

Figure 3. Site−site distribution functions involving NMA oxygen (O) and oxygen (O_w) and hydrogen (H_w) atoms of water as a function of pressure (top panel) for systems S1 (left) and S4 (right) and also as a function of TMAO concentration (bottom panel) for 1 (left) and 8000 (right) atm pressures. Color codes are as in Figure 1.

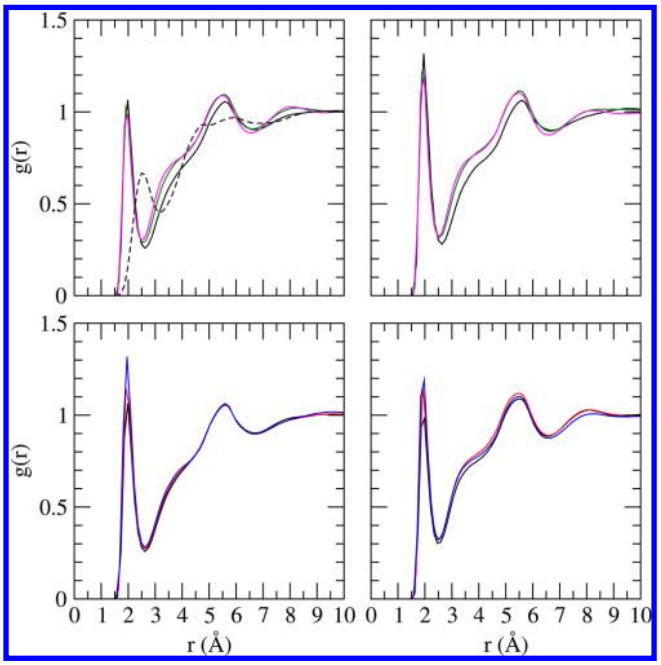

Figure 4. Site−site distribution functions involving NMA hydrogen (H) and water oxygen (O_w) as a function of pressure (top panel) for systems S1 (left) and S4 (right) and also as a function of TMAO concentration (bottom panel) for 1 (left) and 8000 (right) atm pressures. Color codes are as in Figure 1. The dashed line is for water hydrogen (H_w).

water shells surrounding hydrogen bonding sites. In fact, it has been reported that although exposure of hydrophobic groups to water is highly favored under pressure, high pressures have little effect on the tendency of a protein to form hydrogen bonds.[64] Enhanced hydration of these hydrogen bonding sites at high pressure can be inferred from Table 3. TMAO leads to enhancement of first peak (Figures 3 and 4) and removes water molecules from the solvation shell (Table 3), indicating its counterbalancing effect against pressure.

The structural, energetic, and dynamical properties of NMA−water hydrogen bonds were investigated for further characterization of NMA hydration. Following some of our previously published works,[63,65] we defined a hydrogen bond by imposing cutoff distances of r_{DA} for D−A (where D is donor and A is acceptor) and r_{AH} for A−H, and a simultaneous cutoff angle of 45° for H−D−A. Note that the cutoff distances were determined from the positions of the first minimum in the corresponding radial distribution functions at 1 atm for pure water system. To investigate hydrogen bond dynamics, we defined a continuous hydrogen bond correlation function, S_{HB}, as

$$S_{HB}(t) = \langle h(0)\, H(t)\rangle / \langle h\rangle \tag{3}$$

where h and H are hydrogen bond population variables and the angular brackets denote an average over all hydrogen bonds that are present at $t = 0$. If a particular tagged pair of particles is hydrogen bonded (according to the definition adopted above) at time t, h is unity, and is zero otherwise. In case of H, if the tagged pair of particles remains continuously hydrogen bonded from initial period to time t, it takes a value of unity, and is zero otherwise. Clearly, S_{HB} describes the probability that a pair of particles, which was hydrogen bonded initially, remains continuously bonded up to time t. The time integral of S_{HB}, denoted as τ_{HB}, describes the average time that a hydrogen bond survives after it is chosen at $t = 0$. Because the hydrogen bonds are chosen randomly without imposing any condition on when they were created, τ_{HB} is the average persistence time (life expectancy) of a randomly chosen hydrogen bond.

The average number of NMA−water hydrogen bonds per NMA molecule at different conditions chosen are presented in Table 4 together with their energies and lifetimes. Some points are particularly interesting to be noted here. (a) In the presence of water only, NMA oxygen can form about 1.7 hydrogen bonds with water which is about 2 times larger than the average number of NH···O_wH_w bonds. The hydrogen bond lifetime is also much smaller for the latter, although these hydrogen bonds are approximately isoenergetic. (b) For both types of hydrogen bonds, hydrogen bond number increases with increasing pressure and the attractive interaction reduces. Unlike these similar trends for number and energy, the hydrogen bond lifetime follows opposite trend with pressure reducing lifetime of CO···H_wO_w bond and enhancing NH···O_wH_w bond lifetime. Influence of pressure on hydrogen bond properties is, however, not very significant. (c) TMAO reduces the number of NMA−water hydrogen bonds, makes these hydrogen bonds energetically attractive, and enhances their lifetimes. The carbonyl oxygen shows higher sensitivity to the presence of TMAO. Corroborative evidence for higher lifetime of CO···H_wO_w hydrogen bond as compared to that of NH···O_wH_w and TMAO-induced enhancement of these hydrogen bonds can be seen in Figure 5, which illustrates slower relaxation of S_{HB} with time.

To present the effects of TMAO on hydrogen bond energy under high pressure conditions, the probability distributions of NMA−water hydrogen bond energies are shown in Figures 6 and 7. We first notice that the distribution is not uniform with the maximum probability at about −23 kJ mol^{-1} for CO···H_wO_w and NH···O_wH_w hydrogen bonds for the system

dx.doi.org/10.1021/jp311102v | J. Phys. Chem. B 2013, 117, 677−689

Table 4. NMA–Water Hydrogen Bond Properties[a]

		O–H_w			H–O_w		
system	P (MPa)	n_{HB}	E_{HB}	τ_{HB}	n_{HB}	E_{HB}	τ_{HB}
S1	0.1	1.69	−20.02	1.20	0.75	−19.64	0.71
S1	200	1.74	−19.73	1.18	0.79	−19.20	0.72
S1	400	1.75	−19.45	1.13	0.82	−18.94	0.84
S1	600	1.74	−19.26	1.11	0.83	−18.78	0.87
S1	800	1.80	−18.97	1.00	0.88	−18.31	0.94
S2	0.1	1.55	−20.30	1.53	0.75	−19.86	0.79
S2	200	1.58	−20.02	1.53	0.77	−19.41	0.87
S2	400	1.57	−19.79	1.45	0.79	−18.94	0.91
S2	600	1.60	−19.53	1.42	0.82	−18.70	0.94
S2	800	1.60	−19.35	1.31	0.83	−18.56	0.96
S3	0.1	1.42	−20.48	1.75	0.69	−20.07	0.88
S3	200	1.51	−20.22	1.65	0.74	−19.41	0.91
S3	400	1.51	−19.97	1.54	0.77	−19.09	0.97
S3	600	1.43	−19.69	1.66	0.74	−18.81	1.09
S3	800	1.49	−19.48	1.60	0.79	−18.63	1.18
S4	0.1	1.35	−20.75	1.91	0.70	−20.09	0.88
S4	200	1.38	−20.38	1.95	0.71	−19.62	1.03
S4	400	1.43	−20.03	1.90	0.76	−19.10	1.06
S4	600	1.46	−19.80	1.79	0.78	−18.74	1.08
S4	800	1.45	−19.74	1.59	0.81	−18.57	1.18

[a] n_{HB}, E_{HB}, and τ_{HB} represent average number, energy (kJ mol^{-1}), and lifetime (ps), respectively.

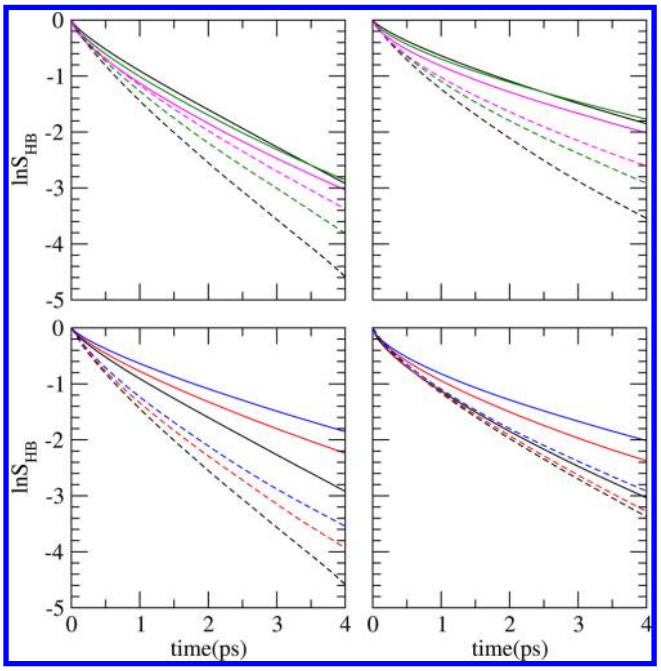

Figure 5. Time dependence of the continuous NMA–water hydrogen bond correlation function, S_{HB}, as a function of pressure (top panel) for systems S1 (left) and S4 (right) and also as a function of TMAO concentration (bottom panel) for 1 (left) and 8000 (right) atmospheric pressures. Color codes are as in Figure 1. Solid and dashed lines are for CO···H_wO_w and NH···O_wH_w hydrogen bonds, respectively.

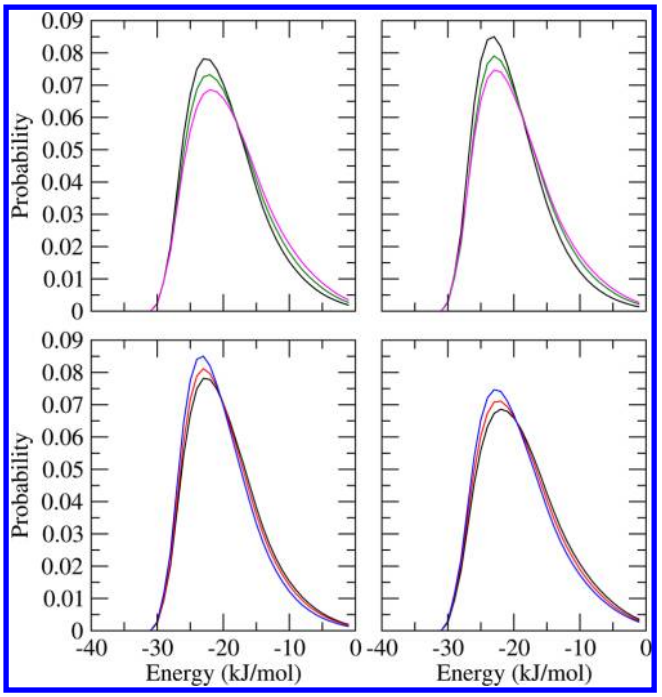

Figure 6. Probability distribution of CO···H_wO_w hydrogen bond energies as a function of pressure (top panel) for systems S1 (left) and S4 (right) and also as a function of TMAO concentration (bottom panel) for 1 (left) and 8000 (right) atm pressures. Color codes are as in Figure 1.

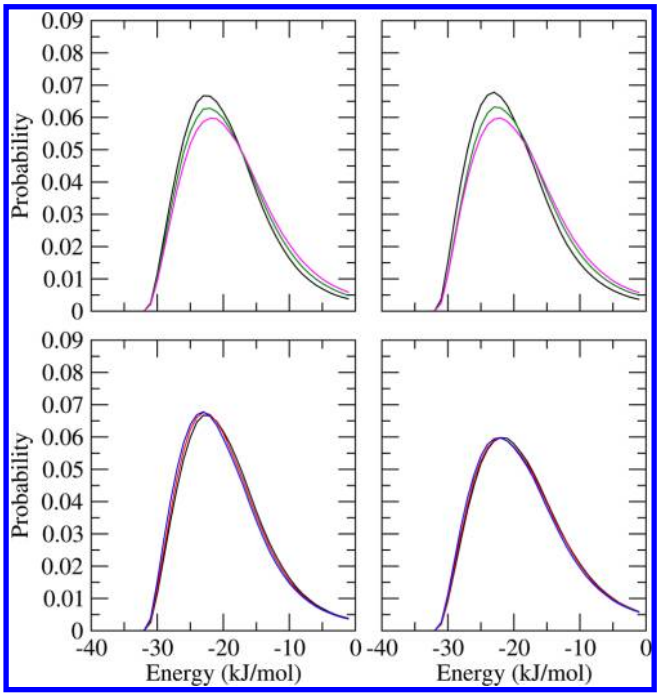

Figure 7. Probability distribution of NH···O_wH_w hydrogen bond energies as a function of pressure (top panel) for systems S1 (left) and S4 (right) and also as a function of TMAO concentration (bottom panel) for 1 (left) and 8000 (right) atm pressures. Color codes are as in Figure 1.

with pure water at 1 atm. Also, the energy distribution is relatively broader for amide hydrogen bond. Clearly, applied pressure increases the probability in the low energy (less negative) region and at the same time, decreases probability in the high energy (more negative) region. Therefore, the evidence here is that NMA–water hydrogen bonds are destabilized at high pressure. Figure 6 shows that TMAO stabilizes hydrogen bonds between carbonyl oxygen and water. This is indicated by higher probabilities in the high energy

dx.doi.org/10.1021/jp311102v | J. Phys. Chem. B 2013, 117, 677–689

region and lower probabilities in the low energy region compared to those with the pure water system. However, energy distribution of NH···O_wH_w hydrogen bond changes barely when TMAO is added to the system.

Thus a thorough investigation of the hydration characteristics of different atomic sites in NMA in pure water and in aqueous solutions of TMAO at different pressure conditions reveals that application of high pressure leads to significant compression of hydration layers of hydrophobic groups and the number of water molecules in the vicinity of both nonpolar groups and hydrogen bonding sites increases. Some new hydrogen bonds between NMA and water start to form, and the relative population of weaker hydrogen bonds increases at the extreme pressure condition. TMAO, on the other hand, can offset the pressure-induced enhanced hydration of NMA atomic sites. It reduces number of NMA−water hydrogen bonds, makes these hydrogen bonds energetically stronger and also slows down the decay of these hydrogen bonds with time. All these findings are consistent with protein denaturation at high pressure and TMAO-induced counteraction. Two possible ways to investigate the underlying mechanism by which protein hydration is influenced by TMAO under high pressure conditions are to examine the direct interaction of TMAO with protein residues (which eventually competes with water) and also the indirect effect of TMAO on water structure. In the following, we have discussed both of these two possibilities in aqueous NMA solutions at different environments.

B. Direct interaction of TMAO with NMA. Selected radial distribution functions between atomic centers of NMA and TMAO are shown in Figure 8. For system S2 at 1 atm, the rdf between the TMAO carbon (C_t) and the carbonyl methyl group (Me_1) in NMA has a first peak at about 3.9 Å with peak magnitude 1.4. Similar observations are made for amide methyl group (Me_2) in NMA. These show that TMAO can interact directly with hydrophobic residue through its methyl groups. Although there is a tendency of O_t to form hydrogen bonds with amide N, the hydrogen bond number between peptide and TMAO is very small for all systems chosen (see Figure 1 in Supporting Information). Note that lack of hydrogen bonding sites for TMAO in peptide backbone have been suggested in a number of studies.[32,66] Though TMAO was shown to form only 0.1 hydrogen bonds with amide N for glycine peptides (2−5 residues),[66] 1.2 hydrogen bonds were found between TMAO and the fully extended configuration of a decaalanine peptide.[32] Similarly, less than 0.5 peptide−TMAO hydrogen bond per structure was found for the pentadecaglycine by Hu et al.[19]

To examine the solvation of NMA more closely, we calculated a preferential binding parameter, $\tau_{w/t}$, using the relation

$$\tau_{w/t}(r) = \frac{n_w(r)}{n_t(r)} - \frac{N_w}{N_t} \quad (4)$$

where $n(r)$ is the number of molecules at a particular distance around NMA atomic sites and N represents the total number of molecules in the system with subscripts w and t standing for water and TMAO molecules, respectively. This binding parameter measures the local ratio of water to TMAO minus their bulk ratio and, hence, gives deviation from an ideal solvation model. A negative value of $\tau_{w/t}$ indicates preferential interaction of TMAO over water and its positive value indicates

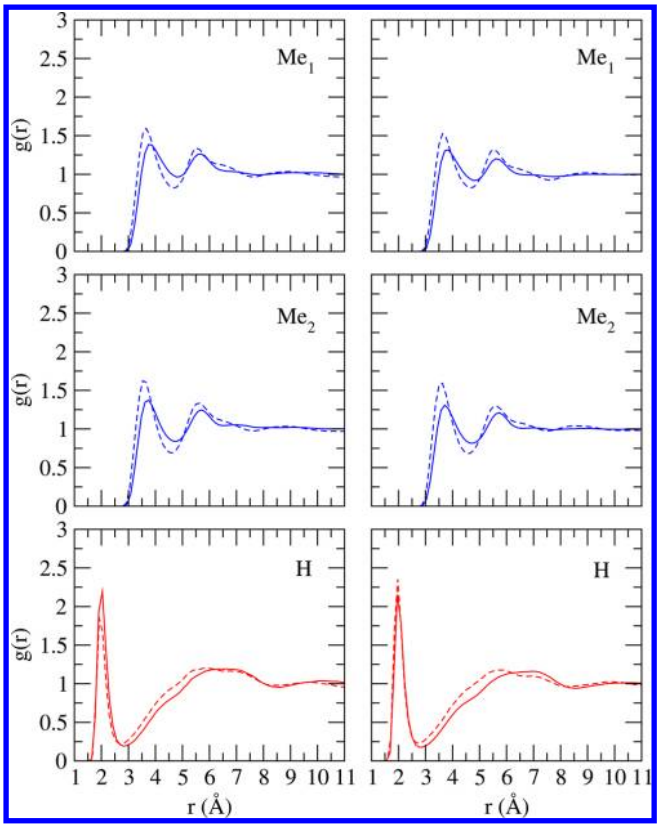

Figure 8. NMA−TMAO site−site distribution functions for systems S2 (left) and S4 (right) at 1 (solid line) and 8000 (dashed line) atm pressures. Red and blue lines are for TMAO oxygen (O_t) and carbon (C_t), respectively.

preferential hydration or preferential exclusion of TMAO in that region.

Figure 9 shows the $\tau_{w/t}$ values around carbonyl methyl group as a function of distance. Because TMAO is a significantly larger molecule than water, it has to be excluded from a certain volume shell around Me_1 for purely geometric reasons, and this is reflected in positive numerical values of $\tau_{w/t}$ at shorter distances. For system S2 at 1 atm, the local ratio is equal to the bulk ratio at about 4.2 Å. The $\tau_{w/t}$ value then starts to decrease with distance, reaches a minimum at about 4.8 Å, and eventually gets its ideal value at longer distances. In a previous simulation study by Hu et al., preferential exclusion of TMAO below 4 Å was observed for a model peptide length of fifteen glycines.[19] Clearly, increasing pressure makes the solvation layers more pronounced. Preferential exclusion of TMAO now creates increased water hydration layer around NMA sites and vice versa. On the contrary, for a particular pressure, the solvation layers are better mixed in terms of water and TMAO at high concentration of TMAO.

Hence, TMAO is found to be excluded preferentially from the local region of Me_1 and similarly of Me_2 and amide *N* (not shown). However, preferential exclusion of TMAO does not suggest that it has no tendency to interact with NMA atomic centers. The term "preferential exclusion" only indicates that the number ratio of TMAO and water molecules is lower in the vicinity of NMA than that in the bulk. TMAO does interact with NMA atomic sites through its methyl groups and oxygen atom. The existence of TMAO interaction sites in the vicinity of NMA sites can be expected to reduce hydration number of these sites, as observed in coordination number analysis.

dx.doi.org/10.1021/jp311102v | J. Phys. Chem. B 2013, 117, 677−689

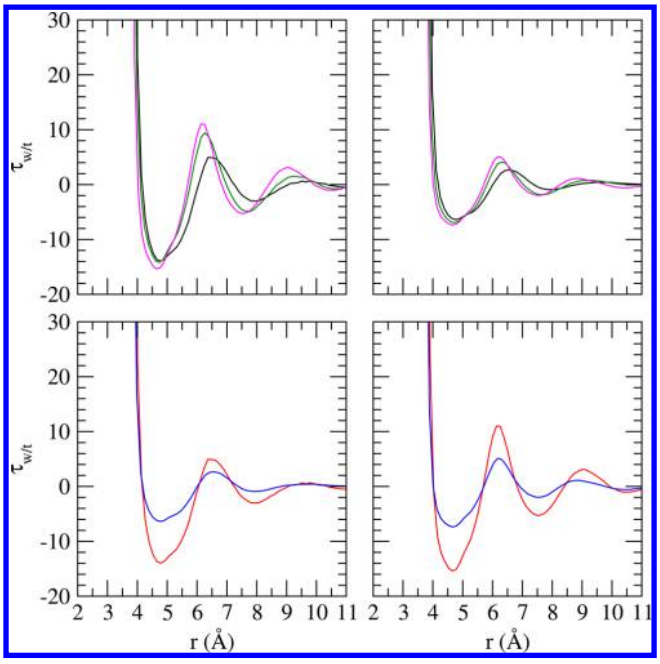

Figure 9. Preferential interaction parameter around carbonyl methyl group as a function of pressure (top panel) for systems S2 (left) and S4 (right) and also as a function of TMAO concentration (bottom panel) for 1 (left) and 8000 (right) atm pressures. Color codes are as in Figure 1.

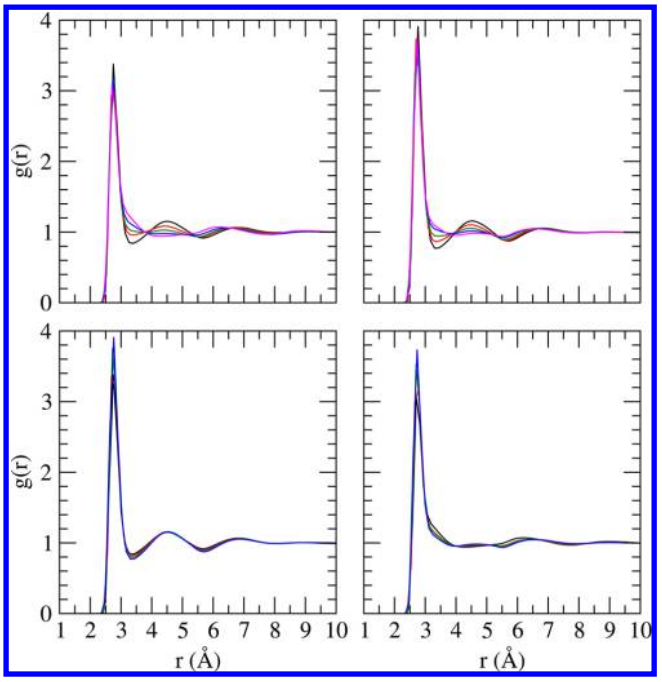

Figure 10. Water oxygen−oxygen site−site distribution functions as a function of pressure (top panel) for systems S1 (left) and S4 (right) and also as a function of TMAO concentration (bottom panel) for 1 (left) and 8000 (right) atm pressures. Color codes are as in Figure 1.

C. Effect of TMAO on Water Properties. It has been suggested in the literature that TMAO can interact strongly with water to form di- and/or trihydrated TMAO complexes in solution.[13,22−25] In a recent study, we examined the behavior of water molecules in the vicinity of both hydrophobic (methyl) and hydrogen bonding (oxygen) sites in TMAO as a function of its concentration at different pressures.[67] TMAO molecules were found to be well solvated by water molecules at ambient pressure conditions. Number of hydrogen bonded water molecules to TMAO oxygen enhanced slightly at high pressure. Moreover, total number of TMAO−water hydrogen bonds increased with increasing concentration of TMAO. We pointed out that the number of water molecules required to solvate all TMAO molecules present in the system increases at high TMAO contents.[67] The data shown in Figures 2 and 3 in Supporting Information confirm those observations.

To shed light on the indirect effect of TMAO solvation on water properties, we examined the structural and dynamical properties of water at different pressure conditions with increasing concentration of TMAO.

In Figure 10, we have shown water−water (O_w−O_w) rdf as a function of pressure as well as of TMAO concentration. In pure water at 1 atm, the first and second peaks, which characterize the hydrogen bonded first neighbor and the tetrahedrally located second neighbor, appear at about 2.8 and 4.5 Å, respectively. On average, 4.7 identical neighbors are found for each water molecule by integrating the rdf to 3.4 Å (location of first minimum in the rdf). The average coordination number of water in the bulk was reported as 5.2 at 1 atm and 300 K.[68] Considering the fact that the number reduces in the vicinity of a large solute,[68] and 20 large NMA molecules are present in our simulation system, the coordination number observed here agree quite well with that study.

There is a remarkable influence of pressure on water structure. To be specific, though the first peak does not show any significant pressure sensitivity, the changes in the first minimum (3.4 Å) and the second peak (4.5 Å) are easy to notice. These observations are consistent with both experiments[51] and computer simulations[51,69] and are clear indicators for movement of part of the water molecules in the second shell toward the first shell, filling the empty spaces in this region. Thus, the first shell of water is crowded at high pressure and there is a collapse of second water hydration shell.

The counteracting effect of TMAO on pressure-induced water structure modification is reflected in Figure 10. TMAO enhances the first peak and makes the first valley deeper. The first and second water shells are, therefore, more defined in the presence of TMAO. In other words, TMAO enhances water structure. Experimental and molecular dynamics simulation studies indicated the ability of TMAO to serve as "water structure maker" at 1 atm.[22,23,25−31,70−72] It is important to be quite clear that this water structure making property of TMAO is equally valid under high pressure conditions (see bottom-left panel in Figure 10).

The pressure and TMAO concentration dependence of the local structure of water is elucidated further by tabulating the average number (N_H) of water oxygen around water oxygen within a shell of 3.4 Å for all simulated systems (Table 5). The enhancement in the number of identical neighbors in the first shell of water can be seen immediately in this table. We observe that, in the presence of water but in the absence of TMAO, the coordination number increases from 4.67 at 1 atm to 6.33 at 8000 atm (an increase of about 35%). Table 5 also reveals that TMAO reduces the number of near neighbor water molecules. There is a decrease of coordination number by 20% at 1 atm as we move from pure water system (4.67) to the system containing 40 TMAO molecules (3.75). The decrease of coordination number for these two systems is found to be 29% at 8000 atm.

dx.doi.org/10.1021/jp311102v | J. Phys. Chem. B 2013, 117, 677−689

Table 5. Average Number of Water Oxygen around Water Oxygen within a Shell of 3.4 Å and Water−Water Hydrogen Bond Properties[a]

system	P (MPa)	N_H	n_{HB}	E_{HB}	τ_{HB}
S1	0.1	4.67	3.52	−19.17	1.25
S1	200	5.29	3.60	−18.80	1.23
S1	400	5.35	3.64	−18.54	1.21
S1	600	5.48	3.72	−18.28	1.18
S1	800	6.33	3.74	−18.07	1.19
S2	0.1	4.20	3.35	−19.41	1.47
S2	200	4.71	3.44	−19.14	1.51
S2	400	4.80	3.48	−18.85	1.52
S2	600	4.90	3.48	−18.65	1.51
S2	800	5.56	3.54	−18.45	1.49
S3	0.1	4.15	3.32	−19.53	1.60
S3	200	4.67	3.37	−19.28	1.66
S3	400	4.75	3.40	−19.02	1.65
S3	600	4.86	3.43	−18.78	1.66
S3	800	4.95	3.46	−18.61	1.65
S4	0.1	3.75	3.20	−19.73	1.77
S4	200	4.17	3.25	−19.44	1.82
S4	400	4.69	3.29	−19.19	1.81
S4	600	4.83	3.31	−19.02	1.88
S4	800	4.89	3.36	−18.82	1.89

[a] N_H, n_{HB}, E_{HB}, and τ_{HB} represent average coordination number of water, average number of hydrogen bonds, energy (kJ mol^{-1}), and lifetime (ps), respectively.

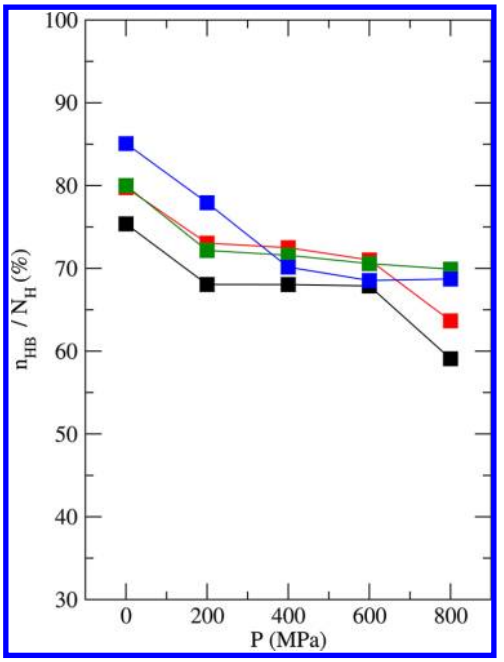

Figure 11. Fraction of hydrogen bonded water molecules in the radial shell of 3.4 Å as a function of pressure for systems S1 (black), S2 (red), S3 (green), and S4 (blue).

To probe the changes in water properties further, we performed an analysis of structural and dynamical properties of water hydrogen bond network at different pressure conditions for aqueous solutions in the presence and absence of TMAO.

Table 5 depicts the average number, energy, and lifetime of water−water hydrogen bonds for all systems considered. Among the 4.67 first shell water molecules in pure water at 1 atm, 75% (n_{HB} = 3.52) are hydrogen bonded to the central water molecule. The water−water average hydrogen bond energy is about −19 kJ mol^{-1}, which is weaker than those between NMA and water by about 1 kJ mol^{-1}. In addition, though the lifetime of water−water hydrogen bond (1.25 ps) is similar to that of CO···H_wO_w (1.20 ps), it is much higher than that of NH···O_wH_w (0.71 ps). High pressure increases the number of hydrogen bonds, as expected from increased water crowding. For example, in the absence of TMAO, average hydrogen bond number increases from 3.52 to 3.64 and then to 3.74 as pressure increases from 1 through 4000 to 8000 atm. Slight reduction in hydrogen bond energy and lifetime of these hydrogen bonds are observed at high pressure. It is important to emphasize that the fraction (n_{HB}/N_H) of hydrogen bonded water molecule in the first shell decreases at high pressure (Figure 11). For the maximum pressure chosen, this decrease is found to be about 0.16. So, although number of nearest identical neighbors per water molecule increases at high pressure with consequent increase in average hydrogen bond number, a relatively higher fraction of first shell water molecules do not participate in these hydrogen bonds. This feature of water under high pressure is likely why pressure increases hydration of NMA molecules and, extended to proteins, leads to water penetration. Transferring water from its (water) first shell allows them to move freely in the bulk, giving an entropic profit to the system; and at the same time, it does not disturb water hydrogen bond network much (less energy loss). Our results are consistent with the notion that translational entropy relaxation in bulk water is an important factor in water penetration and consequent protein denaturation at high pressure.[47−49]

Focusing on the influence of TMAO on water hydrogen bonding network, we find a reduced number of hydrogen bonded water molecules. A few additional points that are of importance are TMAO makes hydrogen bonds more attractive, leads to a slower relaxation of water hydrogen bond network, and enhances the fraction (n_{HB}/N_H) of hydrogen bonded water molecule in the first shell at a particular pressure (Figure 11). At 1 atm, the difference in fraction of hydrogen bonded water molecule between systems S1 and S4 is 0.10. Thus, TMAO shows a tendency to increase the fraction of hydrogen bonded water molecules. Because the first shell water molecules are largely associated through strong hydrogen bonds in the presence of TMAO, the penalty of removing a water molecule from the water solvation shell will increase (due to large energy loss) and, hence, the NMA hydration process will be decelerated. The reduced number of hydrogen bonded water molecules in the presence of TMAO can be viewed in terms of less number of first shell water molecules. Previous simulation study by Zou et al. showed water structure enhancement by TMAO in the form of a slight increase in the number of water−water hydrogen bonds per water molecule,[22] whereas the data obtained by Pettitt and his co-workers demonstrated no evidence for an increase in the water hydrogen bonding structure caused by the addition of TMAO.[19,32] Though our hydrogen bond analysis agree with the results obtained by Pettitt and his co-workers, it also suggests that TMAO does enhance water hydrogen bonding network by increasing fraction of hydrogen bonded first shell water molecules and making these hydrogen bonds stronger.

Slight changes in water−water hydrogen bond lifetime at high pressure and TMAO-induced enhancement of the same is reflected in the slight change in the hydrogen bond correlation

dx.doi.org/10.1021/jp311102v | J. Phys. Chem. B 2013, 117, 677−689

function (S_{HB}) with time with increasing pressure and much slower decay of this function in the presence of TMAO, as displayed in Figure 12. The probability distributions of water−water hydrogen bond energies are shown in Figure 13. Pressure-induced destabilization of water hydrogen bonding network and the counteracting effect of TMAO can be suggested immediately from this figure. We observe that probability of water−water hydrogen bonds with high energy (more negative) reduces on application of pressure and more and more low energy (less negative) hydrogen bonds form under such conditions. When TMAO is added to the system, the energy distribution shift toward higher energy side, indicating hydrogen bond network stabilization by TMAO.

In Figure 14, we have shown the variation of fraction of water molecules (f_n with n number of hydrogen bonds) as a function of TMAO concentration as well as of pressure. In the absence of TMAO, most of the water molecules are 3- and 4-coordinated and there are small fractions of 2- and 5-coordinated water molecules. Applied pressure increases the fraction of 5-coordinated water molecules and reduces the fraction of 2- and 3-coordinated water molecules. The observed pressure-induced enhancement of higher coordinated water molecules is in excellent agreement with previous Monte Carlo simulation results for methane−water system at different pressures.[73] An opposite effect of TMAO can be seen in this figure. It reduces number of higher coordinated (4 and 5) water molecules and increases fraction of 2- and 3-coordinated water molecules. Thus, water molecules are mostly separated in the presence of TMAO and, as discussed later, this is due to the solvation of large TMAO molecules. Note that, to accommodate a solute, water must create a cavity first that is associated with alteration of water hydrogen bonding network. Although a small molecule can be accommodated easily without any significant perturbation of hydrogen bond network, water cannot maintain this network in the presence of a large solute and loses higher coordinated identical neighbors. The

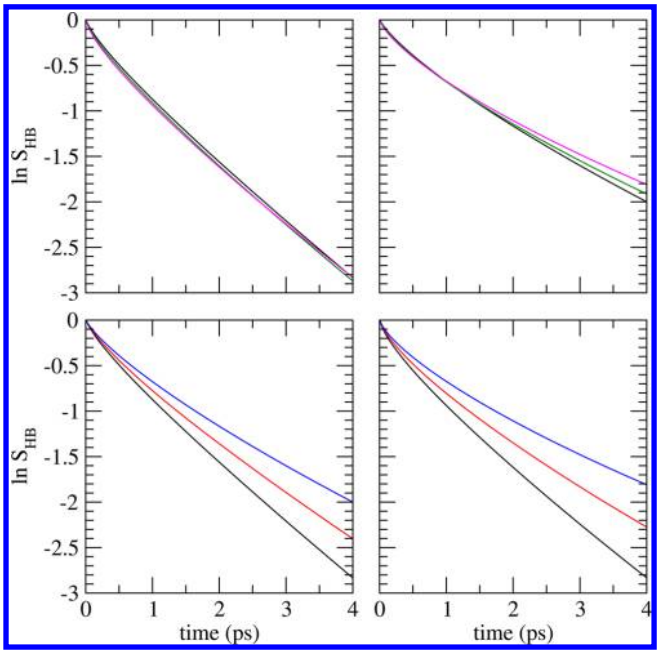

Figure 12. Time dependence of the continuous water−water hydrogen bond correlation function, S_{HB}, as a function of pressure (top panel) for systems S1 (left) and S4 (right) and also as a function of TMAO concentration (bottom panel) for 1 (left) and 8000 (right) atm pressures. Color codes are as in Figure 1.

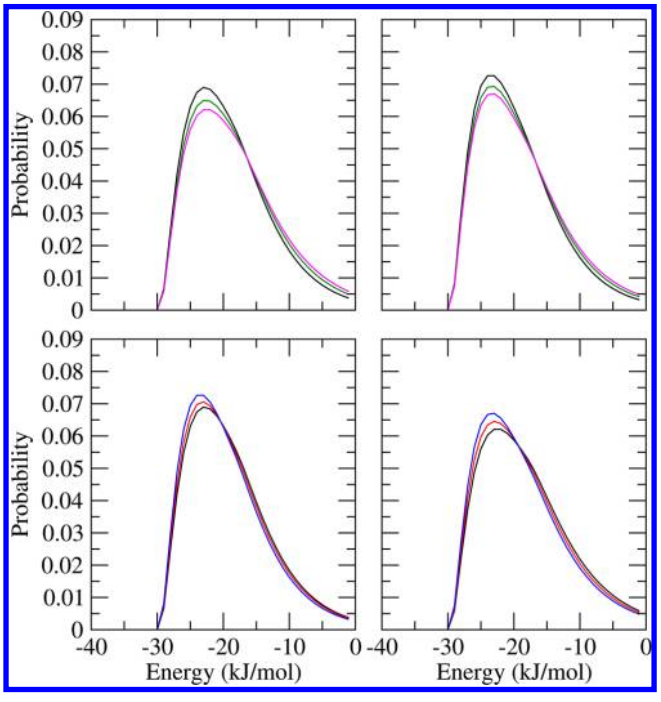

Figure 13. Probability distribution of water−water hydrogen bond energies as a function of pressure (top panel) for systems S1 (left) and S4 (right) and also as a function of TMAO concentration (bottom panel) for 1 (left) and 8000 (right) atm pressures. Color codes are as in Figure 1.

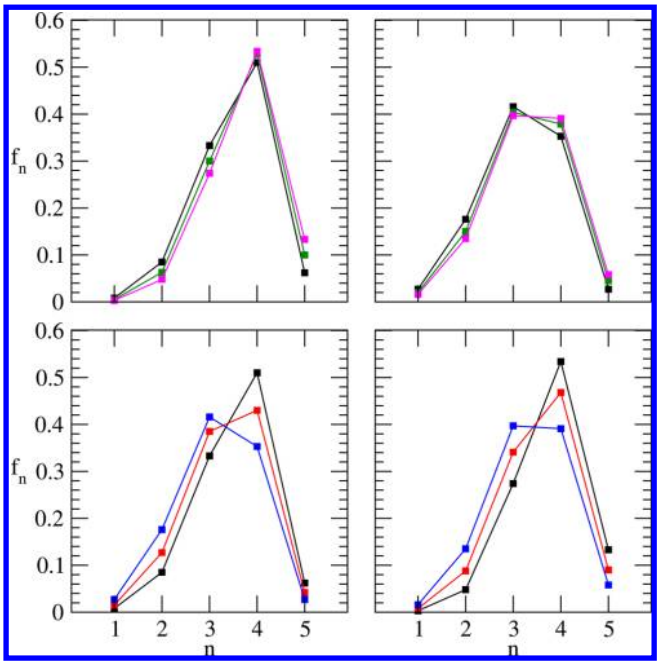

Figure 14. Fraction of water molecules with "n" number of hydrogen bonds with identical species as a function of pressure (top panel) for systems S1 (left) and S4 (right) and also as a function of TMAO concentration (bottom panel) for 1 (left) and 8000 (right) atm pressures. Color codes are as in Figure 1.

dx.doi.org/10.1021/jp311102v | J. Phys. Chem. B 2013, 117, 677−689

effect was discussed in a recent study.[63] The total number of water molecules that solvate TMAO increases with increasing TMAO concentration and this is reflected in enhancement of lower coordinated water molecules with reduction of higher coordinated water molecules with increasing TMAO concentration.

IV. SUMMARY AND CONCLUSIONS

Employing the MD simulation technique, hydration characteristics of hydrophobic and hydrogen bonding sites in NMA were investigated in aqueous solutions of increasing TMAO concentration each at five different pressures ranging from 1 to 8000 atm. The goal of this study was to understand the mechanism of protein protection by TMAO under high pressure conditions. Computations of site−site rdfs indicated that water molecules prefer a surface-parallel orientation in the vicinity of methyl groups but display significant orientational polarizations near the peptide linkage with NMA oxygen showing preference to water hydrogen in its close proximity, whereas oxygen of water is preferred in the solvation shell of NMA hydrogen. The following observations were made at high pressure: (a) In the vicinity of the hydrophobic group, water molecules move from the large-*r* side of the first shell toward its short-*r* side, filling empty spaces in this region and, at the same time, making the hydration shell more defined. (b) The behavior is different near the hydrogen bonding sites in that part of the hydration water is transferred to the large-*r* side of the first shell. These observations are consistent with the suggestion that the water shell is much more compressed in the vicinity of nonpolar groups as compared to that of hydrogen bonding sites[74,75] and also with the notion that, although exposure of hydrophobic groups to water is highly favored under pressure, high pressure has little effect on the tendency of a protein to form hydrogen bonds.[64] TMAO did not affect the water distribution much. Nonetheless, the hydration number of NMA sites that showed enhancement at high pressure was found to be smaller upon addition of TMAO. Solvation characteristics of NMA sites were further explored in terms of NMA−water hydrogen bonds imposing geometric criteria. It was observed that the number of hydrogen bonds formed by NMA oxygen with water is about 2 times larger than that by NMA hydrogen and although these hydrogen bonds have similar energy, the hydrogen bond relaxation is much slower for the former. Pressure-induced enhancement in hydrogen bond number and its reduction in the presence of TMAO were found. It was evident from analysis of hydrogen bond energy distribution that pressure destabilizes NMA−water hydrogen bonds, whereas TMAO increases population of more stable hydrogen bonds. TMAO was also seen to slow down the decay of NMA−water hydrogen bonds. All these results revealed counteracting effect of pressure and TMAO on NMA hydration.

To shed light on the counteracting mechanism, we then examined interaction of TMAO with NMA and the structural and dynamical properties of water at different pressure conditions with increasing concentration of TMAO. TMAO was found to interact directly with NMA atomic sites through its methyl groups and oxygen atom. Significant changes in water structure were observed both at high pressure and in the presence of TMAO. In particular, water molecules in the second shell were transferred to the first shell under high pressure conditions, leading to collapse of the second water shell and enhancement in the number of nearest neighbor water molecules. High pressure enhanced the number of nearest identical neighbors per water molecule with a consequent increase in the average hydrogen bond number. The number of higher coordinated (5) water molecules was found to increase with a reduction in the number of lower coordinated (2 and 3) water molecules. The findings that the relative number of water molecules that do not participate in hydrogen bonding increases and the population of more stable hydrogen bonds reduces with increasing pressure were of significant interest. These findings suggest that water molecules are crowded at high pressure with a relatively destabilized hydrogen bond network. On the contrary, TMAO influenced water properties in a manner that opposes the effects of pressure. Compared to that for pure water, the first and second shells of water were found to be more defined in the presence of TMAO. TMAO not only reduced number of nearest identical neighbors of water but also enhanced the relative number of first shell water molecules that participate in water hydrogen bond network. In addition, the population of more stable hydrogen bonds was found to increase upon addition of TMAO and hydrogen bonds relaxed slowly in these systems, which agree with other simulation findings that TMAO enhances water−water hydrogen bond lifetime.[26] The effects of pressure and TMAO on water properties are thus consistent with their role on NMA hydration.

We mention here that the observed water crowding at high pressure with some "free" water molecules and a relatively destabilized hydrogen bond network explains the reason behind water penetration into the protein interior at high pressure. Due to extreme water crowding, there is a definite entropic loss in the system. The hydrogen bonding network of water is also weaker under these conditions. Water penetration gives an overall entropic profit (due to relaxation in water movement) to the system and allows water to form a relatively stable hydrogen bond network. Note that the dominating contribution of translational entropy gain from relaxation of water molecules far away from the protein surface in overall entropic gain in the system upon pressure denaturation was suggested in the literature.[47] Extending to counteracting pathway of TMAO, TMAO can protect proteins at high pressure by modifying water structure. Because TMAO does not form a hydrogen bond with backbone oxygen and it is difficult to maintain the mandatory solvation sites (two to three) of TMAO oxygen in hydrogen bonding interaction with protein residues, a relatively large fraction of TMAO molecules stay away from the protein surface. Solvation of TMAO molecules by water in the bulk prevents pressure-induced crowding of water molecules (in terms of identical neighbors). This indirect effect of TMAO on water structure greatly reduces the need of water molecules to penetrate into the protein interior. In addition to its effect on water crowding, TMAO also makes the water hydrogen bond network stronger, which increases the penalty of transferring water molecules from its hydrogen bonded network to the interior of the protein. Hence, it is reasonable to conclude that the counteracting effect of TMAO and pressure on the water structural properties play a crucial role in the ability of TMAO to offset protein denaturation under high pressure conditions.

In this study, we have addressed the solvation characteristics of NMA, which represents solvent-exposed state of proteins. Because proteins are much richer than their backbones and pressure denaturation of proteins is associated with elimination of internal cavities and voids, more systematic studies with proteins will be needed for a better understanding of

counteracting mechanism of TMAO against the pressure denaturation of proteins. Furthermore, we carried out MD simulations with the widely used Kast model of TMAO. Recently, it was shown that the Kast model underestimates the osmotic pressure at higher concentrations of TMAO.[76] Although the distinct trends of the effect of TMAO on the water structural and dynamical properties (as compared to pure water) are well captured in our study, use of more realistic TMAO models might prove to be interesting to clarify in details the effects of TMAO at high pressure.

■ ASSOCIATED CONTENT

Supporting Information

NMA−NMA and NMA−TMAO hydrogen bond number as a function of pressure as well as of TMAO concentration. TMAO carbon−water oxygen and TMAO oxygen−water hydrogen site−site rdfs. TMAO−water hydrogen bond number per TMAO oxygen. This information is available free of charge via the Internet at http://pubs.acs.org.

■ AUTHOR INFORMATION

Corresponding Author

*Electronic address: sandipp@iitg.ernet.in.

Notes

The authors declare no competing financial interest.

■ ACKNOWLEDGMENTS

The financial supports of Council of Scientific and Industrial Research (CSIR) and Department of Science and Technology (DST), Govt. of India are gratefully acknowledged.

■ REFERENCES

(1) Lin, T.-Y.; Timasheff, S. N. *Biochemistry* **1994**, *33*, 12695.
(2) Auton, M.; Bolen, D. W. *Proc. Natl. Acad. Sci.* **2005**, *102*, 15065.
(3) Gluick, T. C.; Yadav, S. *J. Am. Chem. Soc.* **2003**, *125*, 4418.
(4) Tatzelt, J.; Prusiner, S.; Welch, W. *EMBO J.* **1996**, *15*, 6363.
(5) Brown, C.; Hong-Brown, L. Q.; Welch, W. *Bioenerg. Biomembr.* **1997**, *29*, 491.
(6) Yancey, P. H. *J. Exp. Biol.* **2005**, *208*, 2819 and references therein.
(7) Daggett, V. *Chem. Rev.* **2006**, *106*, 1898 and references therein.
(8) Venkatesu, P.; Lee, M.-J.; Lin, H.-m. *J. Phys. Chem. B* **2009**, *113*, 5327.
(9) Krywka, C.; Sternemann, C.; Paulus, M.; Tolen, M.; Royer, C.; Winter, R. *Chem. Phys. Chem.* **2008**, *9*, 2809.
(10) Schroer, M. A.; Zhai, Y.; Wieland, D. C. F.; Sahle, C. J.; Nase, J.; Paulus, M.; Tolan, M.; Winter, R. *Angew. Chem., Int. Ed.* **2011**, *50*, 11413.
(11) Hovagimyan, K. G.; Gerig, J. T. *J. Phys. Chem. B* **2005**, *109*, 24142.
(12) Cho, S. S.; Reddy, G.; Straub, J. E.; Thirumalai, D. *J. Phys. Chem. B* **2011**, *115*, 13401.
(13) Rösgen, J.; Jackson-Atogi, R. *J. Am. Chem. Soc.* **2012**, *134*, 3590.
(14) Wang, A.; Bolen, D. W. *Biochemistry* **1997**, *36*, 9101.
(15) Courtenay, E. S.; Capp, M. W.; Anderson, C. F.; Record, M. T., Jr. *Biochemistry* **2000**, *39*, 4455.
(16) Bolen, D. W.; Baskakov, I. V. *J. Mol. Biol.* **2001**, *310*, 955.
(17) Aburi, M.; Smith, P. E. *J. Phys. Chem. B* **2004**, *108*, 7382.
(18) Shimizu, S. *Proc. Natl. Acad. Sci.* **2004**, *101*, 1195.
(19) Hu, C. Y.; Lynch, G. C.; Kokubo, H.; Pettitt, B. M. *Proteins* **2010**, *78*, 695.
(20) Athawale, M. V.; Dordick, J. S.; Garde, S. *Biophys. J.* **2005**, *89*, 858.
(21) Sarma, R.; Paul, S. *J. Phys. Chem. B* **2012**, *116*, 2831.
(22) Zou, Q.; Bennion, B. J.; Daggett, V.; Murphy, K. P. *J. Am. Chem. Soc.* **2002**, *124*, 1192.
(23) Paul, S.; Patey, G. N. *J. Am. Chem. Soc.* **2007**, *129*, 4476.
(24) Stirnemann, G.; Hynes, J. T.; Laage, D. *J. Phys. Chem. B* **2010**, *114*, 3052.
(25) Hunger, J.; Tielrooij, K.-J.; Buchner, R.; Bonn, M.; Bakker, H. J. *J. Phys. Chem. B* **2012**, *116*, 4783.
(26) Bennion, B. J.; Daggett, V. *Proc. Natl. Acad. Sci.* **2004**, *101*, 6433.
(27) Yang, L.; Gao, Y. Q. *J. Am. Chem. Soc.* **2010**, *132*, 842.
(28) Rezus, Y. L. A.; Bakker, H. J. *Phys. Rev. Lett.* **2007**, *99*, 148301.
(29) Qvist, J.; Halle, B. *J. Am. Chem. Soc.* **2008**, *130*, 10345.
(30) Rezus, Y. L. A.; Bakker, H. J. *J. Phys. Chem. B* **2009**, *113*, 4038.
(31) Laage, D.; Stirnemann, G.; Hynes, J. T. *J. Phys. Chem. B* **2009**, *113*, 2428.
(32) Kokubo, H.; Hu, C. Y.; Pettitt, B. M. *J. Am. Chem. Soc.* **2011**, *133*, 1849.
(33) Rossky, P. J.; Karplus, M. *J. Am. Chem. Soc.* **1979**, *101*, 1913.
(34) Pal, S. K.; Zewail, A. H. *Chem. Rev.* **2004**, *104*, 2099.
(35) Bagchi, B. *Chem. Rev.* **2005**, *105*, 3197.
(36) Silva, J. L.; Weber, G. *Annu. Rev. Phys. Chem.* **1993**, *44*, 89.
(37) Hummer, G.; Garde, S.; García, A. E.; Paulaitis, M. E.; Pratt, L. R. *Proc. Natl. Acad. Sci.* **1998**, *95*, 1552.
(38) Balny, C.; Masson, P.; Heremans, K. *Biochim. Biophys. Acta* **2002**, *1595*, 3.
(39) Royer, C. A. *Biochim. Biophys. Acta* **2002**, *1595*, 201.
(40) Paliwal, A.; Asthagiri, D.; Bossev, D. P.; Paulaitis, M. E. *Biophys. J.* **2004**, *87*, 3479.
(41) Lesch, H.; Schlichter, J.; Friedrich, J.; Vanderkooi, J. M. *Biophys. J.* **2004**, *86*, 467.
(42) Paschek, D.; García, A. E. *Phys. Rev. Lett.* **2004**, *93*, 238105.
(43) Collins, M. D.; Hummer, G.; Quillin, M. L.; Matthews, B. W.; Gruner, S. M. *Proc. Natl. Acad. Sci.* **2005**, *102*, 16668.
(44) Day, R.; García, A. E. *Proteins: Struct., Funct., Bioinf.* **2008**, *70*, 1175.
(45) Grigera, J. R.; McCarthy, A. N. *Biophys. J.* **2010**, *98*, 1626.
(46) Imai, T.; Sugita, Y. *J. Phys. Chem. B* **2010**, *114*, 2281.
(47) Harano, Y.; Kinoshita, M. *J. Chem. Phys.* **2006**, *125*, 024910.
(48) Harano, Y.; Yoshidome, T.; Kinoshita, M. *J. Chem. Phys.* **2008**, *129*, 145103.
(49) Yoshidome, T.; Harano, Y.; Kinoshita, M. *Phys. Rev. E* **2009**, *79*, 011912.
(50) Weck, G.; Eggert, J.; Loubeyre, P.; Desbiens, N.; Bourasseau, E.; Maillet, J.-B.; Mezouar, M.; Hanfland, M. *Phys. Rev. B* **2009**, *80*, 180202.
(51) Katayama, Y.; Hattori, T.; Saitoh, H.; Ikeda, T.; Aoki, K. *Phys. Rev. B* **2010**, *81*, 014109.
(52) Schroer, M. A.; Markgraf, J.; Wieland, D. C. F.; Sahle, C. J.; Möller, J.; Paulus, M.; Tolan, M.; Winter, R. *Phys. Rev. Lett.* **2011**, *106*, 178102.
(53) Sarma, R.; Paul, S. *Chem. Phys.* **2012**, *407*, 115.
(54) Berendsen, H. J. C.; Grigera, J. R.; Straatsma, T. P. *J. Phys. Chem.* **1987**, *91*, 6269.
(55) Kast, K. M.; Brickmann, J.; Kast, S. M.; Berry, R. S. R. *J. Phys. Chem. A* **2003**, *107*, 5342.
(56) Jorgensen, W. L.; Swenson, C. J. *J. Am. Chem. Soc.* **1985**, *107*, 569.
(57) Allen, M. P.; Tildesley, D. J. *Computer Simulation of Liquids*; Oxford University Press: New York, 1987.
(58) Berendsen, H. J. C.; Postma, J. P. M.; Gunsteren, W. F.; van; DiNola, A.; Haak, J. R. *J. Chem. Phys.* **1984**, *81*, 3684.
(59) Pratt, L. R.; Chandler, D. *J. Chem. Phys.* **1980**, *73*, 3430.
(60) Trzesniak, D.; Vegt, N. F. A. v. d.; Gunsteren, W. F. v. *Phys. Chem. Chem. Phys.* **2004**, *6*, 697.
(61) Payne, V. A.; Matubayasi, N.; Murphy, L. R.; Levy, R. M. *J. Phys. Chem. B* **1997**, *101*, 2054.
(62) Ghosh, T.; García, A. E.; Garde, S. *J. Am. Chem. Soc.* **2001**, *123*, 10997.
(63) Sarma, R.; Paul, S. *J. Chem. Phys.* **2012**, *136*, 114510.
(64) Randolph, T. W.; Seefeldt, M.; Carpenter, J. F. *Biochim. Biophys. Acta* **2002**, *1595*, 224.
(65) Sarma, R.; Paul, S. *J. Chem. Phys.* **2011**, *135*, 174501.

(66) Hu, C. Y.; Kokubo, H.; Lynch, G. C.; Bolen, D. W.; Pettitt, B. M. *Protein Sci.* **2010**, *19*, 1011.
(67) Sarma, R.; Paul, S. *J. Chem. Phys.* **2012**, *137*, 094502.
(68) Smolin, N.; Winter, R. *J. Phys. Chem. B* **2008**, *112*, 997.
(69) Bagchi, K.; Balasubramanian, S.; Klein, M. L. *J. Chem. Phys.* **1997**, *107*, 8561.
(70) Panuszko, A.; Bruzdziak, P.; Zielkiewicz, J.; Wyrzykowski, D.; Stangret, J. *J. Phys. Chem. B* **2009**, *113*, 14797.
(71) Kuffel, A.; Zielkiewicz, J. *J. Chem. Phys.* **2010**, *133*, 035102.
(72) Wei, H.; Fan, Y.; Gao, Y. Q. *J. Phys. Chem. B* **2010**, *114*, 557.
(73) Chau, P.-L.; Mancera, R. L. *Mol. Phys.* **1999**, *96*, 109.
(74) Smolin, N.; Winter, R. *Biochim. Biophys. Acta* **2006**, *1764*, 522.
(75) Sarupria, S.; Garde, S. *Phys. Rev. Lett.* **2009**, *103*, 037803.
(76) Canchi, D. R.; Jayasimha, P.; Rau, D. C.; Makhatadze, G. I.; Garcia, A. E. *J. Phys. Chem. B* **2012**, *116*, 12095.